Workshop on High Order Methods for CFD - Simulation of Vortex Advection (Case-1.6) Using the Space-Time Discontinuous Galerkin Cell Vertex Scheme (DG-CVS)

Shuangzhang Tu* , Qing Pang† and Haibin Xiang‡

Department of Computer Engineering, Jackson State University
Jackson, Mississippi, 39217, USA

Abstract

In this report, we present the results of the simulation of the vortex transport problem (C-1.6 in the workshop) using a high-order space-time solver based on our discontinuous Galerkin Cell Vertex Scheme (DG-CVS).

1 Code Description

The code used in this study is a high-order space-time solver based on the discontinuous Galerkin Cell-Vertex Scheme (DG-CVS) [1, 2]. The solver is under continuous development since March 2008, under the support from AFOSR Computational Mathematics Program (Grant No. FA9550-08-1-0122 and Grant No. FA9550-10-1-0045).

DG-CVS was inspired by the space-time Conservation Element/Solution Element (CE/SE) [3] method and the discontinuous Galerkin (DG) [4] method. DG-CVS integrates the best features of the two methods. The core idea is to construct a staggered space-time mesh through alternate cell-centered CEs and vertex-centered CEs within each time step. The difference between SEs and CEs is that the SE includes the *volumeless* vertical spike. Inside each SE, the solution is approximated using high-order space-time DG basis polynomials. The space-time flux conservation is enforced inside each CE using the DG discretization. The unknowns are stored at both vertices and cell centroids of the spatial mesh. However, the solutions at vertices and cell centroids are updated at different time levels within each time step successively.

A summary of the main features of DG-CVS is given as follows:

- *based on space-time formulation.* The space-time formulation is advantageous in handling moving boundary problems since it automatically satisfies the Geometric Conservation Law on moving meshes.
- *high-order accuracy in both space and time.* Space and time are handled in a unified way with spacetime flux conservation and high-order spacetime discontinuous basis functions.
- *Riemann solver free.* The Riemann-solver-free feature offers two-fold advantages. First, this Riemann-solver-free approach eliminates some pathological behaviors associated with some Riemann solvers. Second, it is suitable for any hyperbolic PDE systems whose eigenstructures are not explicitly known.
- *reconstruction free.* DG-CVS solves for the solution and its all spatial and temporal derivatives simultaneously at each space-time node, thus eliminating the need of reconstruction.
- *suitable for arbitrary spatial meshes.* The CE and SE definitions in DG-CVS are independent of the underlying spatial mesh and the same definitions can be easily extended from 1-D to higher-dimensions without any ambiguity. The same CE and SE definitions also apply to meshes with hanging nodes [5].

*Corresponding author, Email: shuangzhang.tu@jsums.edu
†Senior Research Associate, Email: qing.pang@jsums.edu
‡Graduate Research Assistant

- *highly compact regardless of order of accuracy.* Only information at the immediate neighboring nodes will be needed to update the solution at the new time level. Compactness eases the parallelization of the flow solver.
- *also accurately solves time-dependent diffusion equations.* In DG-CVS, the inclusion of diffusion terms is straightforward and simple in exactly the same way as how advection terms are handled by simply incorporating the diffusive flux into the space-time flux [2]. No extra reconstruction or recovery or ad hoc penalty and coupling terms are needed to ensure the consistency of the variational form for diffusive terms. For this reason, DG-CVS is conceptually simper than other existing DG methods for diffusion equations.
- *easy nonreflective boundary condition (NRBC) treatment.* The simple NRBC treatment [6] in DG-CVS allows waves to exit the boundary smoothly with little reflection.

DG-CVS offers benefits for both the space-time DG method and the space-time CE/SE method. The benefits for the space-time CE/SE method is two fold. First, DG-CVS increases the CE/SE method's temporal and spatial accuracies by employing high-degree polynomial basis functions inside the SE. Second, DG-CVS presents universal definitions of CEs and SEs for arbitrary meshes. The benefits for the space-time DG method are also two-fold. First, DG-CVS provides a Riemann-solver-free approach for the DG methods. Second, DG-CVS does not need special treatment for the diffusion terms and thus is conceptually simpler than existing traditional DG methods.

2 Case Summary

This study is to test the performance of our DG-CVS solver on the following case

- C1.6: Vortex Transport by Uniform Flow

2.1 Case Description

The domain is rectangular on $[0, L_x] \times [0, L_y] = [0, 0.1] \times [0, 0.1]$ in meters. The domain is first initialized with a uniform flow of pressure $P_\infty = 10^5 N/m^2$, temperature $T_\infty = 300K$ and Mach number $M_\infty = 0.05$, and a vortex of characteristic radius $R = 0.005$ and strength $\beta = 0.02$, is superposed around the center of the domain $(X_c, Y_c) = (0.05, 0.05)$. The vortex is provided via

$$u_0 = U_\infty(1 - \beta\frac{y - Y_c}{R}e^{-r^2/2})$$
$$v_0 = U_\infty\beta\frac{x - X_c}{R}e^{-r^2/2}$$

where

$$r = \sqrt{(x - X_c)^2 + (y - Y_c)^2}/R$$
$$U_\infty = M_\infty\sqrt{\gamma R_{\text{gas}} T_\infty}$$

The temperature and density in the vortex region is prescribed as

$$T_0 = T_\infty - 0.5(\beta U_\infty e^{-r^2/2})^2/C_p$$
$$\rho_0 = \rho_\infty(T_0/T_\infty)^{1/(\gamma-1)}$$

where $\rho_\infty = P_\infty/(R_{\text{gas}}T_\infty)$ and $C_p = \gamma R_{\text{gas}}/(\gamma - 1)$. The pressure inside the vortex $P_0 = \rho_0 R_{\text{gas}} T_0$. The prescribed temperature and density ensure that the vortex is a steady solution of the stagnant flow. Therefore, under uniform background flow, the vortex should be transported horizontally without distortion.

In this case, the ratio of specific heats $\gamma = 1.4$ and the gas constant $R_{\text{gas}} = 287.15 J/kg\,K$. Periodic boundary conditions are assumed on left/right and top/bottom boundaries, respectively.

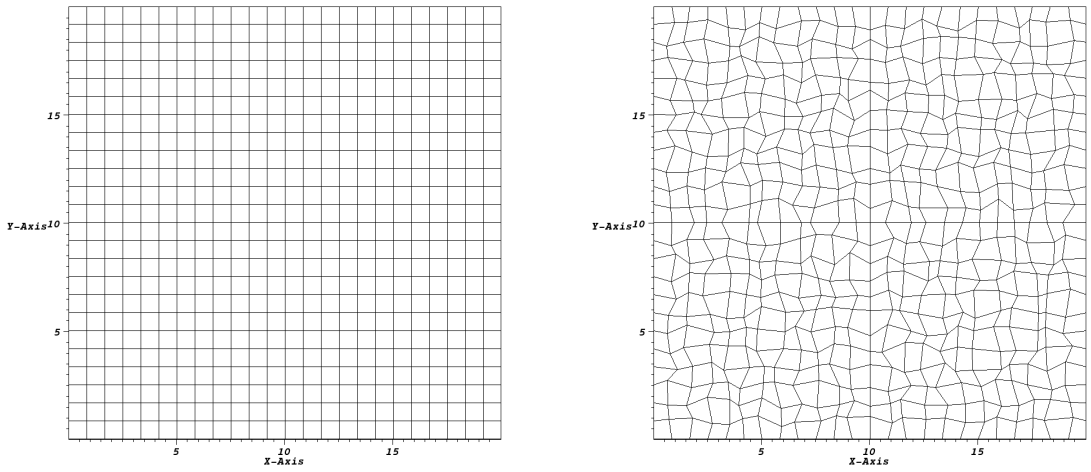

Figure 1: Coarsest meshes used in the case of vortex transport. Left: 24×24 rectangular mesh. Right: randomly perturbed rectangular mesh of the same resolution.

2.2 Residual Tolerances

The L_2 norm of the solution error is evaluated according to

$$||\text{error}||_2 = \sqrt{\frac{\sum_{i=1}^{N} \int_{\Omega_i} (q^h - q^{\text{exact}})^2 \mathrm{d}A}{\sum_{i=1}^{N} \int_{\Omega_i} \mathrm{d}A}}$$

where q^h is the numerical solution and q^{exact} is the exact solution. N is the number of vertices. Appropriate quadrature rule is used to compute the integral.

2.3 Machines Used

All simulations are run on a 64-core Linux cluster. The cluster consists of 16 AMD 2.4 GHz quad-core processors, 128 GB memory, 8TB hard drive storage and infiniband interconnect. Note that the simulation is run in the sequential mode.

3 Meshes Used in the Simulation

The simulations are performed on rectangular meshes and perturbed rectangular meshes with three levels of resolution. The meshes are designated as `qua-24`, `qua-32`, `qua-48`, `qua-24-p`, `qua-32-p` and `qua-48-p` where the numbers are the number of cells in each direction and '`p`' stands for "perturb". The coarsest mesh contains 24×24 cells as shown in Fig. 1.

4 Results

In the simulation, all quantities are nondimensionalized using the following reference values:

$$L_{\text{ref}} = R,\ U_{\text{ref}} = U_\infty,\ \rho_{\text{ref}} = \rho_\infty,\ T_{\text{ref}} = T_\infty \text{ and } P_{\text{ref}} = \rho_\infty U_\infty^2$$

Define the time-period $T = L_x/U_\infty$. The nondimensional period is therefore 20 time units. All the simulations are performed up to 50 periods (i.e. $t = 1000$ time units).

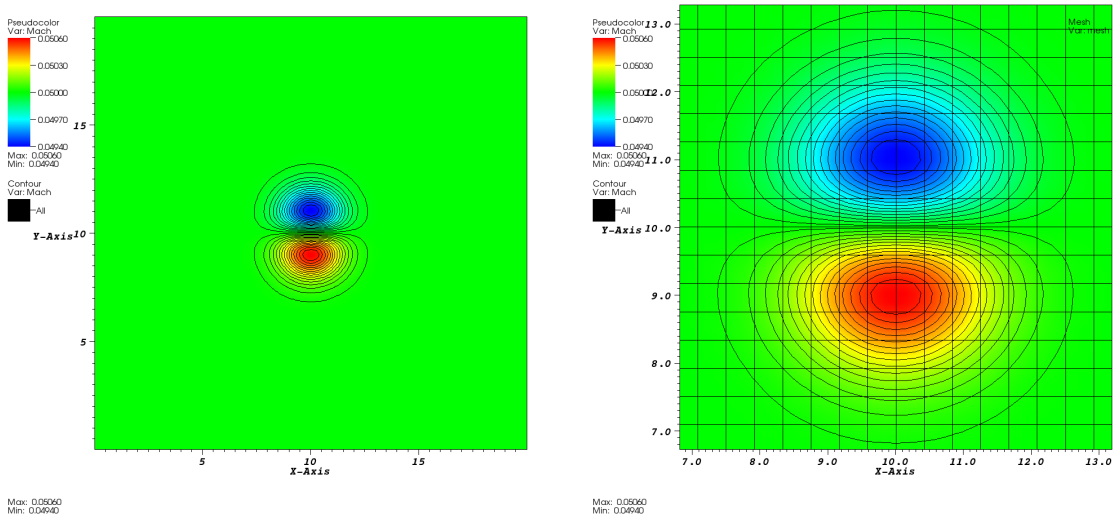

Figure 2: The $p3$ Mach number field at the 50th period on the 48×48 rectangular mesh. Left: entire field. Right: close-up view with grid lines superimposed.

As indicated in the original case guide, the vortex strength β is set to be 0.02. With this β, the density variations is vanishingly small around the vortex.

The fourth order ($p3$) DG-CVS is used in all simulations. The nondimensional time step $\delta t = 0.01$ for the 24×24 rectangular mesh and $\delta t = 0.0075$ for the corresponding perturbed mesh.

4.1 Mach number fields at the 50th period

We first present the field solutions at the end of the 50th period. Figures 2 and 3 shows the Mach number field at the 50th period on the finest meshes (i.e. `qua-48` and `qua-48p`), respectively. As can be seen, the Mach number ranges between 0.0494 and 0.0506. Note that the background uniform flow has the Mach number 0.05.

4.2 Velocity profiles at the 50th period

We first show the velocity profiles along the center lines of the vortex at the 50th period on various meshes. Figure 4 compares the u-component of the velocity along the vertical line $x/R = 10$ for various meshes. Figure 5 compares the v-component of the velocity along the horizontal line $y/R = 10$ for various meshes. As can be seen, the coarse meshes `qua-24` and `qua-24-p` are not able to preserve the velocity profile. By contrast, the fine meshes `qua-48` and `qua-48-p` preserve the profile very well over the long simulation. It can also been observed that the solutions on the regular rectangular meshes are noticeably better than those on the corresponding perturbed meshes.

4.3 L_2 error norms vs. characteristic size

The case guideline requires the L_2 error norms be evaluated on the two components of the velocity vector. The current DG-CVS code outputs error norms on conservative variables instead of primitive variables. In this test case, the density field is nearly constant ($\rho \approx 1$), we expect the error norms based on ρu and ρv reflect the errors norms based on u and v. Table 1 lists the L_2 error norms of x- and y-momentum. In addition, the numerical convergence orders are also determined.

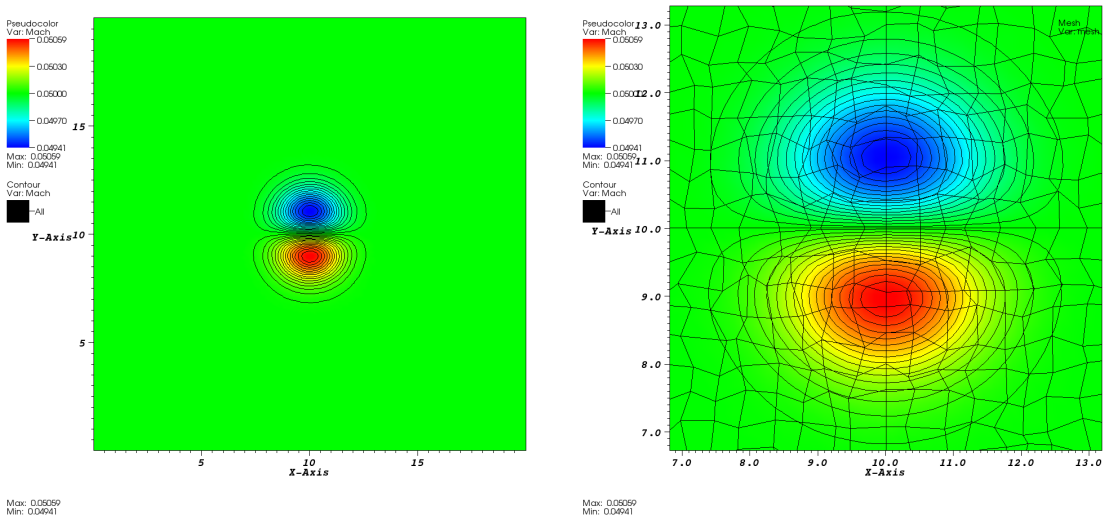

Figure 3: The $p3$ Mach number field at the 50th period on the 48×48 perturbed rectangular mesh. Left: entire field. Right: close-up view with grid lines superimposed.

Table 1: L_2 error norms and the numerical convergence order.

mesh type	mesh	x-momentum		y-momentum	
		$\|\|e\|\|_2$	order	$\|\|e\|\|_2$	order
rectangular	qua-24	3.36E-04	-	3.35E-04	-
	qua-32	1.19E-04	3.61	1.19E-04	3.60
	qua-48	1.40E-05	5.28	1.36E-05	5.35
perturbed quadrilateral	qua-24-p	4.91E-04	-	4.86E-04	-
	qua-32-p	2.14E-04	2.89	2.16E-04	2.82
	qua-48-p	3.67E-05	4.35	3.52E-05	4.47

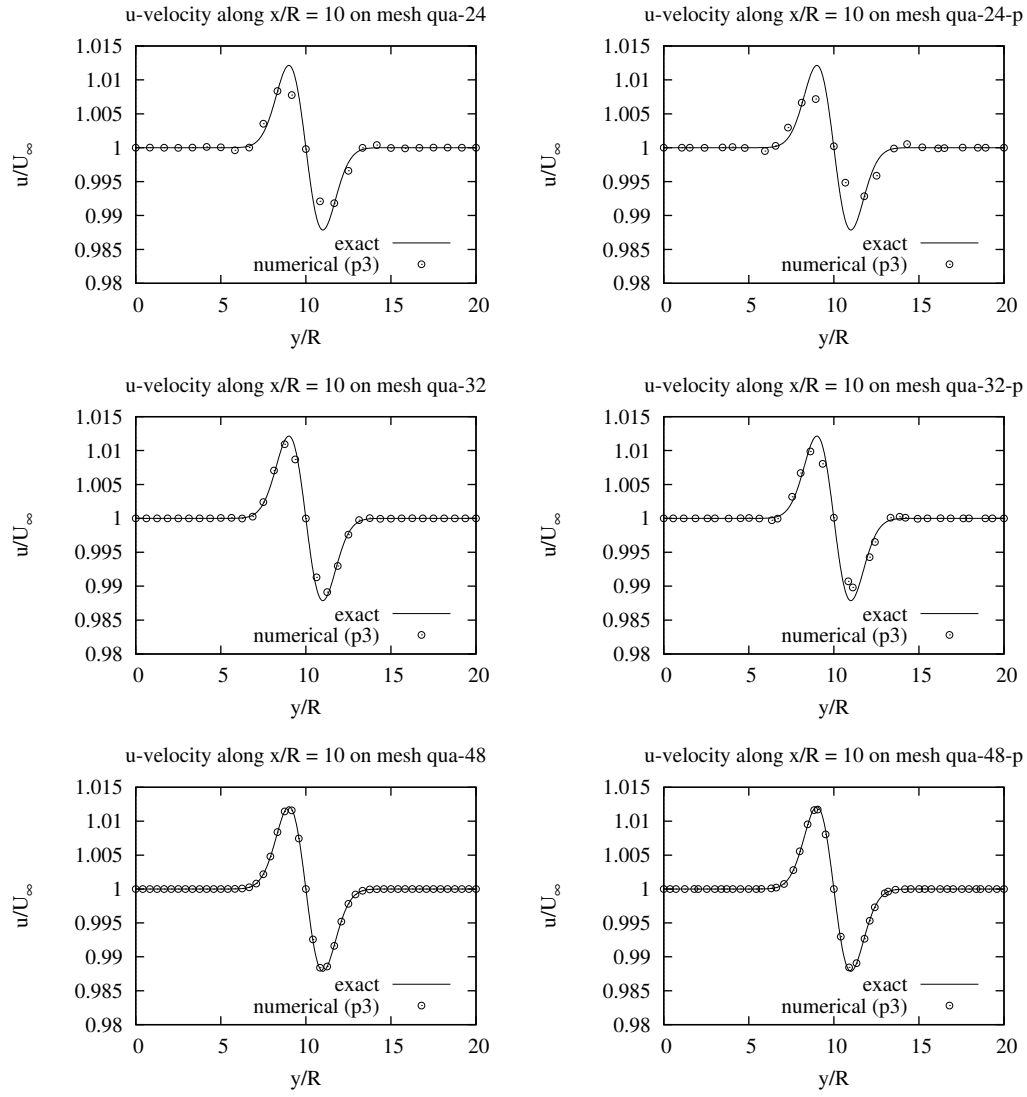

Figure 4: Comparison of the profiles of the u-component of the velocity along the vertical line $x/R = 10$ on various meshes. Left column: rectangular meshes. Right column: corresponding perturbed meshes.

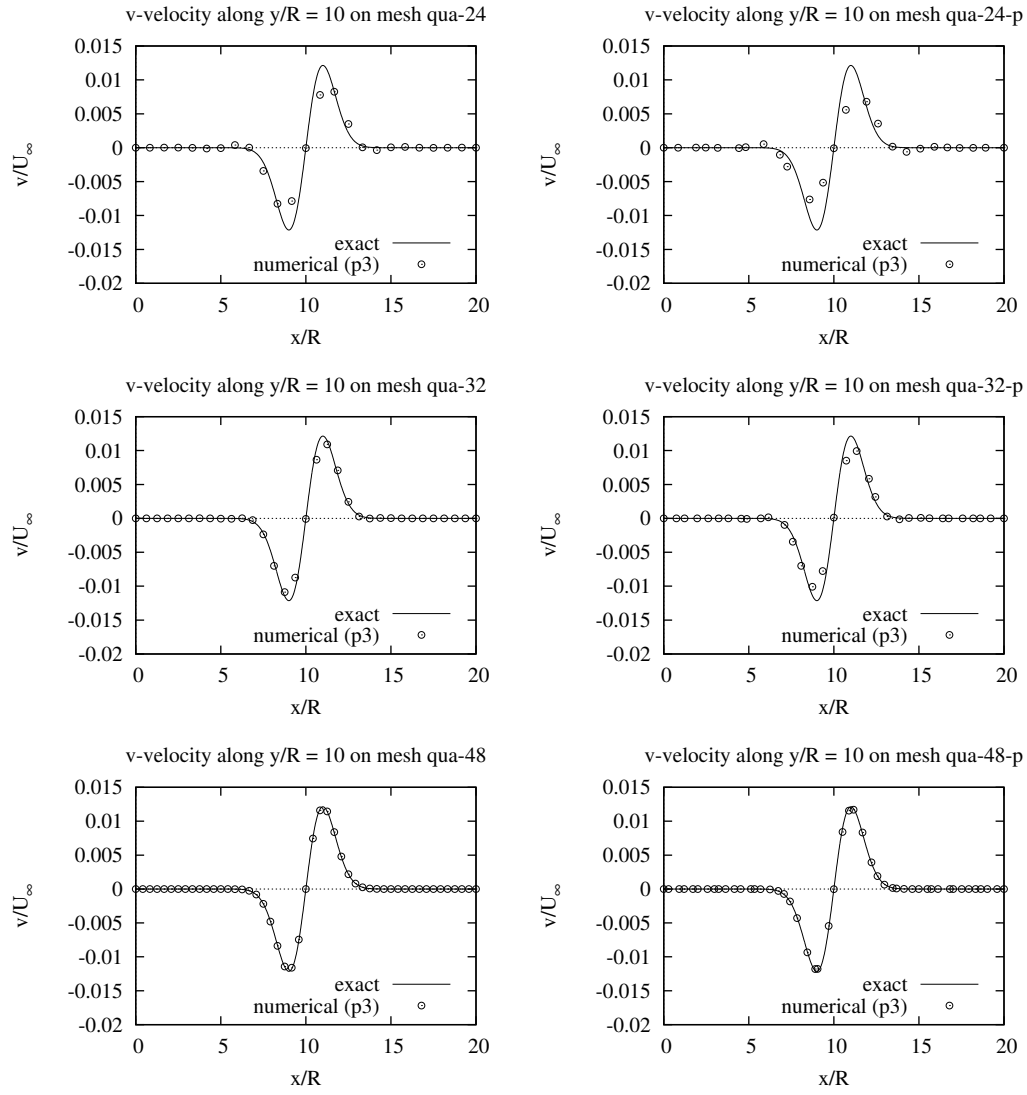

Figure 5: Comparison of the profiles of the v-component of the velocity along the horizontal line $y/R = 10$ on various meshes. Left column: rectangular meshes. Right column: corresponding perturbed meshes.

5 Conclusions

The simulation shows that the $p3$ solutions from the DG-CVS based flow solver are able to preserve the velocity profiles at the 50th period on 48×48 meshes. Besides, the solutions on rectangular meshes are more accurate than those on perturbed meshes. This test demonstrates the accuracy of the high order DG-CVS based solver in preserving weak vortices in low Mach number flows over long-term simulations on relatively coarse meshes. The results also demonstrate the nearly optimal convergence rate of DG-CVS for Euler equations.

Acknowledgments

This work is supported by the U.S. Air Force Office of Scientific Research (AFOSR) Computational Mathematics Program under the Award No. FA9550-08-1-0122 and the Award No. FA9550-10-1-0045. The authors are also grateful to the School of Engineering and the Department of Computer Engineering at Jackson State University for their support.

References

[1] Tu, S., Skelton, G., and Pang, Q., "A compact high order space-time method for conservation laws," *Communications in Computational Physics*, Vol. 9, No. 2, 2011, pp. 441–480.

[2] Tu, S., Skelton, G., and Pang, Q., "Extension of the High-Order Space-Time discontinuous Galerkin Cell Vertex Scheme to Solve Time Dependent Diffusion Equations," *Commun. Comput. Phys.*, Vol. 11, No. 5, 2012, pp. 1503–1524.

[3] Chang, S.-C. and To, W., "A new numerical framework for solving conservation laws: the method of space-time conservation element and solution element," 1991, NASA TM 1991-104495.

[4] Cockburn, B. and Shu, C.-W., "Runge-Kutta discontinuous Galerkin methods for convection-dominated problems," *J. Sci. Comput.*, Vol. 16, No. 3, 2001, pp. 173–261.

[5] Tu, S. and Tian, Z., "Preliminary Implementation of a High Order Space-time Method on Overset Cartesian/Quadrilateral Grids," January 2010, AIAA Paper 2010-0544.

[6] Tu, S., Pang, Q., and Xiang, H., "Wave Computation Using a A High Order Space-time Riemann Solver Free Method," June 2011, AIAA Paper 2011-2846 presented at the 17th AIAA/CEAS Aeroacoustics Conference.